# Dark ice chemistry in interstellar clouds

Qasim, D.N.

# Introduction

## 1.1 The star formation cycle

Our Sun and the planets surrounding it are part of a stellar formation cycle. This cycle starts with the gravitational collapse of a large interstellar cloud and ends after a number of different phases, when the Sun implodes and returns much of its material into the interstellar medium (ISM). Astrochemistry is the research discipline that aims to characterize the involved materials and processes, and to understand how these depend on the many physical and chemical conditions. Much effort has been put into constraining the details of each stage over the years. From an astrochemical perspective, some outstanding questions remain, such as what materials are inherited at each stage of the cycle, and which materials become important to the origin of life on Earth and possibly elsewhere. Therefore, this introduction will outline the current star formation cycle, with added attention to the gas and ice chemistry that is relevant to this thesis research.

Figure 1.1 shows a general schematic of Sun-like star formation. As this thesis focuses on the ISM, an outline of the physical conditions for stages a and b of Figure 1.1 is shown in Table 1.1. At the earliest stage exists the diffuse ISM. This medium consists primarily of atoms, molecules, and ions and is largely ultraviolet (UV)-dominated. It also has very low visual extinction ($A_V$), meaning that the dust and gas densities and columns are low. Here, $A_V$ is best described in relation to the neutral hydrogen atom column: $N_H = 3.08 \times 10^{22} \times A_K$ (Boogert et al. 2013), where $A_V = 8 \times A_K$ (Cardelli et al. 1989). At low densities without sufficient collisions of gas with dust, gas-phase species cannot accumulate to form ices, and thus this medium is driven primarily by gas-phase rather than solid-state chemistry. Even if some ice were to form on the dust grain during this phase, this growth would be hindered by processes such as photodesorption (Watson & Salpeter 1972), which is a process that causes the desorption of species by impacting photons. As the densities increase, a cloud starts to take form. At the edge of the cloud (i.e., the translucent phase), a photon dominated region (PDR) exists that can contain H-, C-, and/or O-bearing simple and complex molecules. Hydrogenation of O, C, and N lead to the formation of simple hydrides, such as $H_2O$, $CH_4$, and $NH_3$, respectively (van de Hulst 1946). More complex species, such as HCOOH, $CH_3CCH$, and $CH_3CHO$, have been observed (Guzmán et al. 2014; Öberg 2016). Traveling deeper into the cloud, the densities increase, resulting in dense clouds ($10^2$ - $10^4$ $H_2$ molecules $cm^{-3}$)

and cores ($10^4$ - $10^5$ $H_2$ molecules $cm^{-3}$). Note that although cores always have high density and high visual extinction, this is not always the case for dense clouds. For background star observations (as will be discussed in section 1.2.3), a sight-line with a high $A_V$ may either have a high density or a low density with a long pathlength. This density increase has a substantial influence on the chemistry that occurs. UV-photons become largely blocked from penetrating the cloud/core, and in combination with the fact that the cooling rates by molecular emission peak, the cloud/core temperature drops to ~10 K. This results in a rich ice chemistry, as the sticking coefficient for all species on micrometer-sized dust grains is unity except for the most volatile atoms and molecules, such as H and $H_2$. Besides chemical reactions on icy dust surfaces, also gas-phase ion-molecule reactions occur (Agúndez & Wakelam 2013). As the observed abundances in the gas phase sometimes cannot be explained by gas-phase mechanisms alone, such as the case for $CH_3OH$ (Garrod et al. 2006; Geppert et al. 2006), it is generally accepted that solid-state reactions are the dominant process. As will be discussed in greater detail in the next section, it is thought that complex organic molecules (COMs; $\geqslant$ 6 atoms and are C and H bearing) primarily originate from this phase in the solid-state. Much is still unclear, however, about the links between solid-state and gas-phase processes.

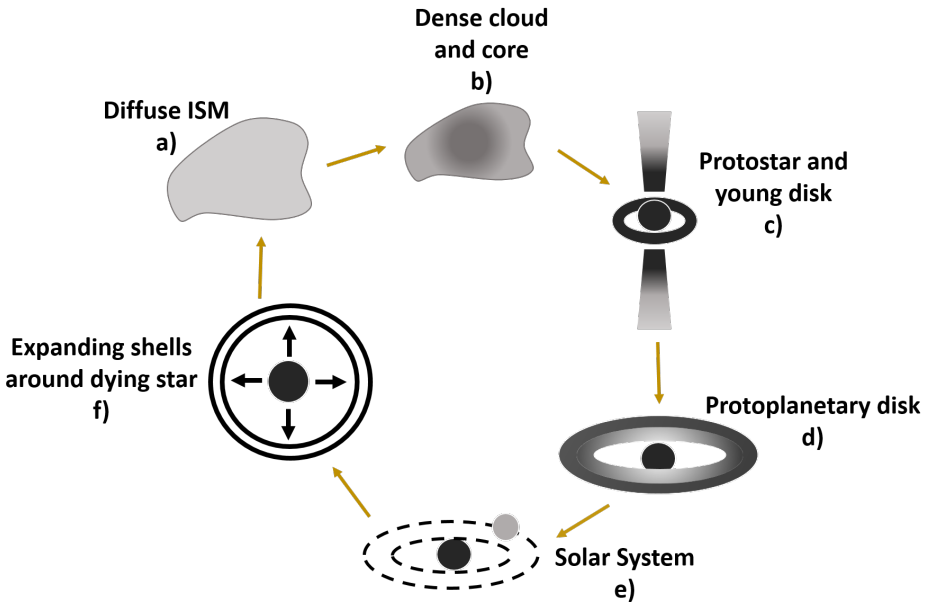


Figure 1.1: The main stages of star formation of a Sun-like star. Adapted from Öberg (2016).

As the dense core increases in mass, its outward pressure becomes less than its inward pressure, and the core eventually collapses under its own gravity (Ward-Thompson 2002). This collapse triggers an increase in the temperature, and at increasing temperatures and densities, a protostar is created, in which it gets most of its luminosity from accretion. Conservation of angular momentum results in an increase in rotation and a decrease in the moment of inertia,

Table 1.1: Physical parameters of the different regions of interstellar clouds, as noted in Table II of van Dishoeck et al. (1993). (a) Dust temperatures are much lower for all noted regions. (b) "Cloud" and "core" are used interchangeably when describing the astrophysical conditions simulated in the experiments presented in this thesis.

| ISM region | Density ($cm^{-3}$) | Gas temperature[a] (K) | $A_V$ (mag) |
|---|---|---|---|
| Diffuse molecular | 100-800 | 30-80 | $\lesssim 1$ |
| Translucent | 500-5000 | 15-50 | 1-5 |
| Dense cloud[b] | $10^2$ - $10^4$ | $\gtrsim 10$ | $\gtrsim$2 |
| Cold, dark core[b] | $10^4$ - $10^5$ | $\approx 10$ | 5-25 |

leading to the formation of a disk and/or outflows (Shu et al. 1987). The starting disk eventually grows in size to form a protoplanetary disk. Observations show that these disks contain organic molecules (Dutrey et al. 1997; Thi et al. 2004; Öberg et al. 2015; Favre et al. 2018; van´t Hoff et al. 2018), although it becomes difficult to probe the less abundant, more complex species (formed in the solid-state), as the spatial scale of disks is relatively small (van´t Hoff et al. 2018). Yet, at early stages, disks are much warmer, and their rich chemical inventory is readily revealed (Jørgensen et al. 2016).

Understanding how the properties of protoplanetary disks link to planet formation is currently (2020) an active field of research. It is theorized that "snow lines", which are regions far enough from the star to allow the freeze-out of gas-phase species (Kennedy & Kenyon 2008), are important to the formation of planets around the new born star. This also applies to our own Solar System. As life exists in our Solar System, detailed knowledge of the many different processes taking place at different locations in a protoplanetary disk, such as better understanding of the role of snow lines in the chemical composition of a disk and in the planet formation process itself, may ultimately show how the building blocks of life arrived on Earth. For example through impacting comets, which are small icy bodies and remnants of the protoplanetary material that carry the chemical memory of the processes in diffuse and dense clouds (Chyba & Sagan 1997; Altwegg et al. 2019). Over time, the star will grow out of the main sequence phase as it becomes depleted of hydrogen, essentially burning up its surroundings. After a number of events involving drastic temperature and pressure changes, for Sun-like stars, its outer layers enhanced in heavy elements will eventually be ejected (Guidry 2019), providing material for the cycle to start over again.

## 1.2 Translucent, dense cloud, and dark core stages

The dense cloud and dark core stages of the star formation cycle and the preceding translucent stage are what this thesis work is based upon. The studies

presented in the next chapters focus on this step in the cosmochemical evolution, largely through dedicated laboratory experiments and extended with astronomical surveys. The most up-to-date astrochemical constraints of this stage that are relevant to this thesis are discussed in the following subsections.

### 1.2.1 Observationally constrained ice phases

As mentioned in section 1.1, the formation of the dense molecular cloud in the star formation cycle results in a rich ice chemistry, as temperatures drop, causing gas-phase species except H and $H_2$ to accrete onto dust grains. These icy dust grains are excellent hosts for chemical reactions to take place, as the surface itself provides a platform for species to congregate, as well as absorbs excess energy from highly exothermic reactions that may cause product dissociation. Astronomical observations show that the ices on grain mantles in interstellar clouds are initially formed in chemical layers, and this layering process is strongly dependent on the dust extinction, or cloud depth (see Boogert et al. (2015) and references therein). A visualization of the first ice phases is shown in Figure 1.2. At a visual extinction ($A_v$) of 1.6 mag, $H_2O$ ice starts to grow by H- and O-atom accretion (Whittet et al. 2001; Ioppolo et al. 2008, 2010; Cuppen et al. 2010), and is the most abundant ice to be detected, with a typical column density of $\sim 10^{18}$ cm$^{-2}$ (see for example, Boogert et al. (2011)). At this point, photodesorption becomes less likely, which allows species that hit the dust to increasingly stay on the dust surface. Other atoms also accrete, such as C and N, and can be hydrogenated to form $CH_4$ (Qasim et al. 2020) and $NH_3$ (Fedoseev et al. 2014), respectively. $CO_2$ is also found in this ice phase, and is likely formed starting from the reaction between CO and OH species (Ioppolo et al. 2011; Garrod & Pauly 2011; Arasa et al. 2013). It has a typical column density of $\sim 10^{17}$ cm$^{-2}$ (see for example, Boogert et al. (2011)). As the density is around $10^3$ cm$^{-3}$ in this phase, mostly atomic species are available with some CO.

At $A_v > 3$, the molecular $H_2$ density increases to $\sim 10^4$ cm$^{-3}$, resulting in a "heavy" CO freeze-out, in which < 50% of the CO freezes out onto icy grain mantles (Chiar et al. 1995). This causes an apolar layer to form on top of the previously formed polar layer. Due to the increase in the density, more diatomics, such as $N_2$ and $O_2$, should become available. At $A_v > 9$, the density reaches $\sim 10^5$ cm$^{-3}$, resulting in a "catastrophic" CO freeze-out (Jørgensen et al. 2005; Pontoppidan 2006). This CO-rich ice is hydrogenated and is collectively found to be the dominating pathway to $CH_3OH$ formation in interstellar molecular clouds (Watanabe & Kouchi 2002; Fuchs et al. 2009; Cuppen et al. 2009; Boogert et al. 2011; Wirström et al. 2011). It is noted, however, that the $CH_3OH$ ice formation threshold still needs further constraints. Additionally, $CH_3OH$ is not always detected at $A_v > 9$, thus Figure 1.2 does not represent all interstellar cloud environments. More details about this phenomenon can be found in Qasim et al. (in preparation; Chapter 5).

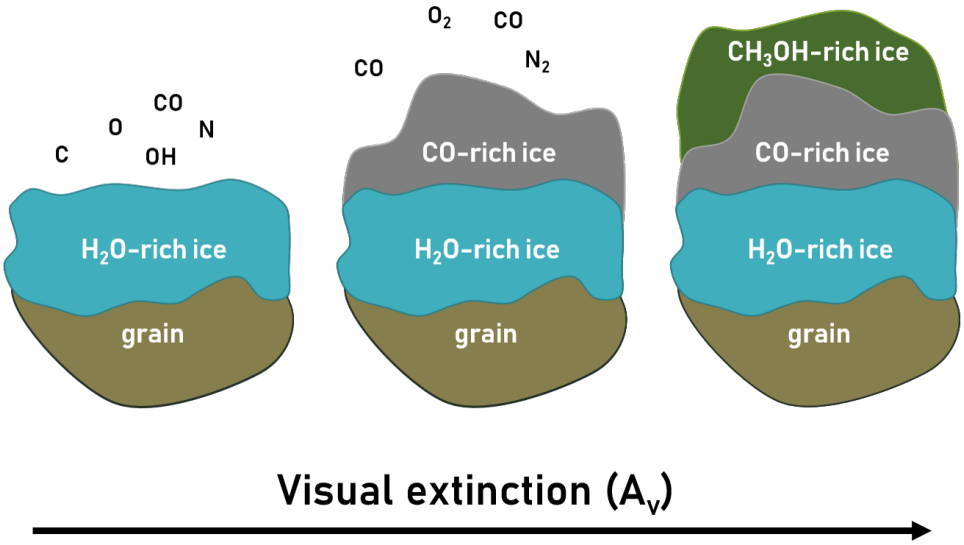


Figure 1.2: The first ice phases, largely as a function of the visual extinction ($A_v$), as constrained by observations. Gas-phase species relevant to the ice chemistry are noted with black font. Adapted from Boogert et al. (2015).

### 1.2.2 Non-energetic and energetic ice chemistry

The formation and destruction of molecules in the solid-state in interstellar clouds are largely governed by two processes: 'energetic' and 'non-energetic'. In this specific context, a 'non-energetic' process refers to "a radical-induced process without the involvement of UV, cosmic rays, and/or other 'energetic' particles" (Qasim et al. 2019d). This is also known as 'dark' chemistry. The emphasis on the process being radical-induced is due to the fact that at the low temperatures of ~10 K, radicals are essential for 'dark' ice chemistry to occur. The relevance of the 'non-energetic' process in dense clouds and dark cores is due to the phenomenon in which certain energy sources, such as external UV-photons, become increasingly blocked by the shroud of dust and gas. Note, however, that the atoms used for 'non-energetic' ice chemistry are largely generated from the gas-phase through 'energetic' processes. For example, cosmic-rays can still penetrate dense regions, which dissociate $H_2$ gas to H-atoms needed for 'non-energetic' solid-state chemistry. Cosmic-rays also cause the production of at least electrons and UV-photons (Herbst & van Dishoeck 2009), which then contribute to 'energetic' processing. A number of laboratory efforts has demonstrated that 'energetic' processing of ices can lead to the formation from simple molecules to biologically relevant species (Allamandola et al. 1988; Caro et al. 2002; Bernstein et al. 2002; Öberg et al. 2009; Materese et al. 2017; Ligterink et al. 2018).

The formation of simple molecules, such as $H_2O$, $NH_3$, and $CH_4$, is primarily due to 'non-energetic' processes, when atomic H, O, N, and C simultaneously accrete (Linnartz et al. 2015). Additionally, the only detected solid-state COM, $CH_3OH$, is predominantly formed by 'non-energetic' processing (see section 1.2.1). Recent laboratory experiments have shown that UV-irradiation of a

$CO:H_2$ ice mixture does lead to the simple radical, HCO (Chuang et al. 2018a). UV-irradiation of molecules, such as $CH_3OH$, also leads to the formation of simple radicals, which can recombine to form rather complex species (Öberg et al. 2009). COMs have been shown to be effectively produced by both, 'energetic' and 'non-energetic' processes (Chuang et al. 2017). When the two processes are combined, radicals that are formed from photolysis become hydrogenated, leading to the formation of simple species in addition to COMs (Chuang et al. 2017). Such COMs include methyl formate, glycolaldehyde, and ethylene glycol – all of which have been detected in observational surveys (Jørgensen et al. 2012).

There are mainly three reaction mechanisms that are considered to take place in interstellar ices: Langmuir-Hinshelwood (L-H), Eley-Rideal (E-R), and Kasemo-Harris (K-H) (Kolasinski 2012). If the reactant species are thermalized with the surface prior to reaction, then the reaction follows an L-H mechanism. If one reactant is thermally equilibrated with the surface and the other is a gas-phase species, then the reaction follows an E-R mechanism. Finally, if one reactant is thermally equilibrated with the surface and the other reactant is on the surface but not fully equilibrated, then the mechanism for reaction is K-H. In this thesis, it is found that the L-H mechanism dominates many of the reactions, as it is found that our H-atoms equilibrate to the temperature of the surface before a reaction is attempted.

As the experiments presented in this thesis typically take place at 10 K and involve atomic hydrogen, it is no surprise that tunneling is an influential aspect for these reactions to proceed. As temperatures drop, the rate constant becomes increasingly dependent on tunneling (Meisner & Kästner 2016). Tunneling is the phenomenon in which a particle has a statistical chance larger than zero to cross an energy barrier. The longer the wavelength of the particle, the more likely it will be able to cross the barrier. From the de Broglie relation, species with the smallest mass will have the greatest wavelength, and this wavelength increases as the temperature decreases (Hama & Watanabe 2013). Thus, at low temperatures of 10 K, atomic hydrogen is the most likely atom to tunnel through a barrier, simply from this perspective. This is observed through a number of reactions studied in this thesis, such as CO + H and $C_2H_2$ + H, which have barriers that are difficult to cross over at 10 K.

### 1.2.3 Ice detections

The most abundant ice to be detected in the ISM is $H_2O$, followed by $CO_2$, CO, $CH_3OH$, $NH_3$, and $CH_4$ (Öberg et al. 2011). Their relative median ice abundances towards low-mass young stellar objects (LYSOs) are shown in Figure 1.3. There are several ways in which ices are observed. In one case, the star acts as a light source while being remote from the cloud/core. In the observer's line of sight, this star is behind the cloud/core, making it a "background" or "field" star. This kind of observation is used to trace pristine ices, since the star does not process the dust grain or ice. However, dark cores can also contain protostars.

Other ways to observe ice features in the infrared are by exploiting embedded protostars (YSOs embedded in the molecular cloud) and OH-IR stars (stars that are bright in the infrared and exhibit strong OH maser emission), as discussed

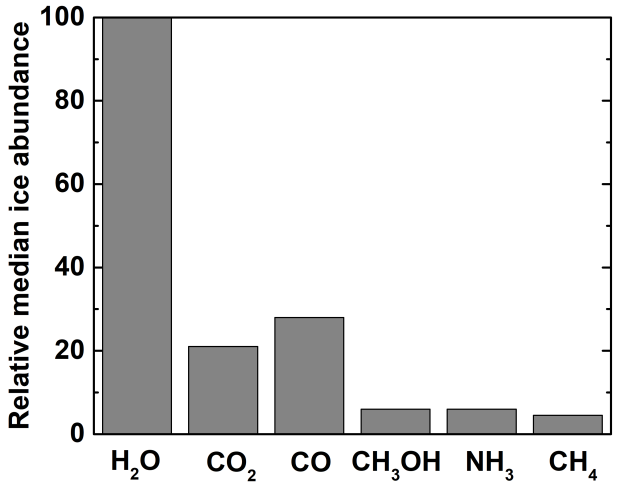


Figure 1.3: Relative median ice abundances of the six most abundant ices detected towards low-mass young stellar objects. Values obtained from Boogert et al. (2015).

in Millar & Williams (1993) and summarized here. Protostars are advantageous in that they are luminous and therefore a good S/N can be achieved, in comparison to background stars, in which their light is more attenuated by the cloud. However with increasing wavelength, the flux decreases, and additionally, the star itself may process the ice. OH-IR stars are unique in that carbon-poor ices can be studied. Their envelopes are oxygen rich, with an elemental C/O < 1. Thus, most of the C is locked-up in CO, as also found in dense clouds and dark cores. Due to the warm temperatures, sticking of CO onto dust grains is inhibited, allowing for ice formation without an abundance of carbon.

In addition to the aforementioned ices, there are also likely identified species (one absorption feature probed and matches laboratory spectra) and possibly identified species (one absorption feature probed and match to laboratory spectra not found; see Boogert et al. (2015) and references therein). These include $H_2CO$, $OCN^-$, and OCS (likely identified), as well as HCOOH, $CH_3CH_2OH$, $HCOO^-$, $CH_3CHO$, $NH_4^+$, $SO_2$, and polycyclic aromatic hydrocarbons (PAH) (possibly identified). Ironically, although there are strong arguments for effective COM formation in the solid-state in dense clouds and dark cores (as discussed in section 1.2.5), $CH_3OH$ is the only COM that has been securely identified directly in the ice. This is, in part, substantially due to the lack of sensitivity provided by previous and current observational facilities, as well as the inherent problem of indistinguishable features in solid-state infrared spectra (Terwisscha van Scheltinga et al. 2018). As will be discussed in the next section, many more COMs have been detected in the gas-phase, in part because gas-phase spectra intrinsically have more resolved features. Additionally, gas-phase spectroscopy can be used to constrain the formation history of detected COMs (i.e., whether they are formed in the solid-state, gas-phase, or

both). For example, Soma et al. (2018) exploit the line profiles of several COMs and compare them to species that are known to be formed in the solid-state (e.g., $CH_3OH$) and gas-phase (e.g., carbon chain molecules). The line shape is influenced by the distribution of the species (e.g., a narrower line width may mean a more compact distribution). Thus if the spectral line shapes are similar, it means that the species spatially co-exist, and are thought to be formed along a similar formation route (i.e., in the solid-phase or gas-phase or even both). Other example efforts to explain the formation history of COMs through the analysis of gas-phase chemistry are demonstrated in Balucani et al. (2015), Jiménez-Serra et al. (2016), and Lee et al. (2019).

### 1.2.4 Gas-phase detections

As shown in Table 1.2, there are many more gas-phase than solid-state detections of COMs in dense clouds and dark cores. However, as discussed by Bacmann et al. (2019), there are still limitations to gas-phase observations of COMs in dense clouds and dark cores. Like in solid-state observations, high sensitivity and lengthy integration times are needed, partially because the low temperatures trap a number of COMs in the solid-state. Regardless, more than a handful of COMs has been detected in these environments.

### 1.2.5 Likelihood of icy complex organic molecules (COMs)

Astrochemical models have shown that gas-phase chemistry alone cannot reproduce the observational abundances of a number of COMs (Herbst & Leung 1989; Millar et al. 1991; Charnley et al. 1992, 1995; Garrod et al. 2006). Thus, the (partial) formation of (certain) COMs in interstellar ices is likely. Solid-state laboratory experiments have pioneered the effort to uncover which COMs can be created in the solid-state under relevant translucent and dark cloud conditions. This is because within the astrochemical 'triangle' that consists of observations, models, and laboratory, specifically experimental laboratory has the advantage to confirm under what conditions species are formed, which is the first piece of information needed to know if such COMs can exist in interstellar ices (as direct ice observations are not currently available).

In the Laboratory for Astrophysics at Leiden Observatory, much dedication has been put into the study of COMs under translucent and dense cloud/dark core conditions, and has further strengthened the argument of COM formation in ices of such interstellar clouds. To do this, an ultrahigh vacuum (UHV) apparatus, SURFace REaction SImulation DEvice (SURFRESIDE), is exploited. This setup allows to somewhat simulate the accretion of atoms, molecules, and molecular fragments in interstellar clouds. Notably, three atomic beamlines are attached to the main vacuum chamber and can collectively produce H-, C-, N-, and O-atoms. These atoms are directed towards a substrate that is typically cooled to 10 K, which is a representative temperature of dust grains in such environments. To our knowledge, this is the only cryogenic UHV apparatus that contains three different atomic beamlines, making it one of the most advanced systems to study the initial formation of interstellar ices. The analytical techniques used to study the ice, reflection-absorption infrared spectroscopy

Table 1.2: A list of COMs that have been detected in the gas-phase in dense clouds and/or dark cores. The reference column lists references in which the detection of the species was first reported. The list of species is predominantly acquired from the census by McGuire et al. (2018).

| Species | Cloud/Core | Reference |
|---|---|---|
| $HC_5N$ | TMC-1 | Kroto et al. (1977) |
| $HC_7N$ | TMC-1 | Kroto et al. (1977) |
| $HC_9N$ | TMC-1 | Broten et al. (1978) |
| $CH_3CCH$ | TMC-1 | Irvine et al. (1981) |
| $CH_3C_4H$ | TMC-1 | Walmsley et al. (1984) |
| $CH_3C_3N$ | TMC-1 | Broten et al. (1984) |
| $CH_3CHO$ | TMC-1 and L134N | Matthews et al. (1985) |
| $C_6H$ | TMC-1 | Suzuki et al. (1986) |
| $CH_3OH$ | TMC1, L134N, and B335 | Friberg et al. (1988) |
| $HC_2CHO$ | TMC-1 | Irvine et al. (1988) |
| $HC_3NH^+$ | TMC-1 | Kawaguchi et al. (1994) |
| $H_2C_6$ | TMC-1 | Langer et al. (1997) |
| $CH_2CCHCN$ | TMC-1 | Lovas et al. (2006) |
| $CH_3C_5N$ | TMC-1 | Snyder et al. (2006) |
| $CH_3C_6H$ | TMC-1 | Remijan et al. (2006) |
| $C_6H^-$ | TMC-1 | McCarthy et al. (2006) |
| $C_8H^-$ | TMC-1 | Brünken et al. (2007) |
| $CH_2CHCH_3$ | TMC-1 | Marcelino et al. (2007) |
| $HCOOCH_3$ | L1689B | Bacmann et al. (2012) |
| $CH_3OCH_3$ | L1689B | Bacmann et al. (2012) |
| $HC_5O$ | TMC-1 | McGuire et al. (2017) |
| $HC_7O$ | TMC-1 | McGuire et al. (2017) |
| $C_6H_5CN$ | TMC-1 | McGuire et al. (2018) |
| c-$C_2H_4O$ | L1689B | Bacmann et al. (2019) |

(RAIRS) and temperature programmed desorption (TPD), are however typical within the fields of astrochemistry and surface science.

An intensive study on $CH_3OH$ formation, with $CH_3OH$ being the simplest COM, within the CO + H reaction pathway was performed by Fuchs et al. (2009), and first demonstrated by Watanabe & Kouchi (2002). This pathway, which becomes relevant in the CO freeze-out stage (see section 1.2.1), has also been shown to be promising for the formation of larger COMs. The study by Fedoseev et al. (2015) showed that the simultaneous deposition of CO and H can also lead to the formation of glycolaldehyde and ethylene glycol, and has the potential to form ribose, which is an essential component of ribonucleic acid. Adding $H_2CO$ to the mixture, which is a CO hydrogenation product, results in the additional formation of methyl formate (Chuang et al. 2016). Starting from glycolaldehyde, glycerol and glyceraldehyde can be formed (Fedoseev et al. 2017).

The reaction of $C_2H_2$ + CO + H was investigated in the work by Qasim et al. (2019a), as $C_2H_2$ can be hydrogenated to form $C_2H_x$ radicals, which can react to form a unique set of COMs. The $C_2H_2$ + CO + H reaction network derived from the experimental work of Qasim et al. (2019a) is shown in Figure 1.4. Within the orange square-dotted circle are the radicals and their recombination products in the CO + H reaction network, as constrained from the laboratory experiments by Chuang et al. (2016). In Qasim et al. (2019a), $C_2H_2$ and its hydrogenated counterparts were added to the network. The saturated radicals ($C_2H_3$ and $C_2H_5$) can react with HCO from the CO + H network to form aldehydes (propanal and propenal) and an alcohol (propanol).

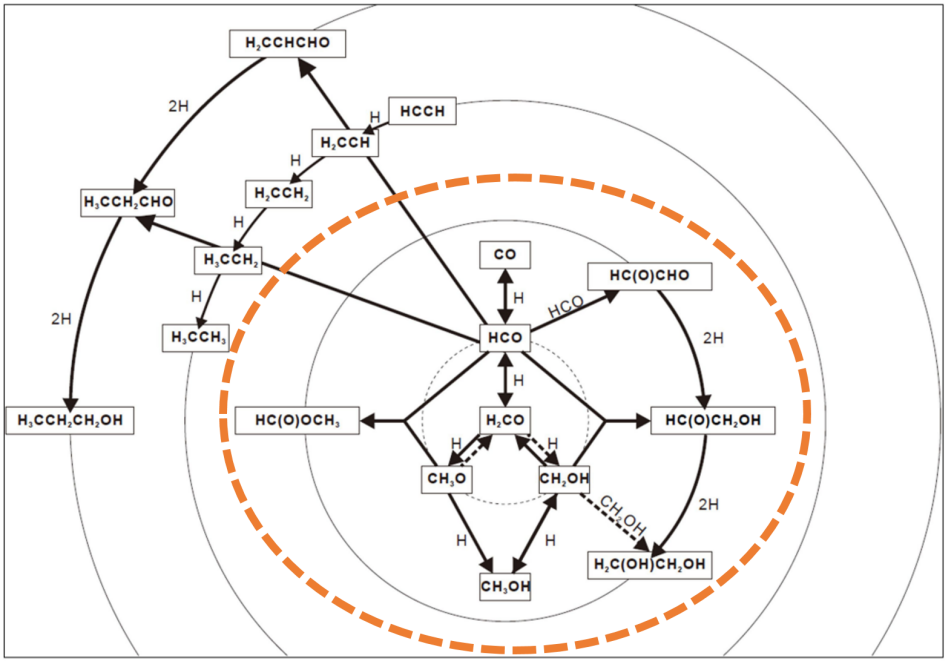


Figure 1.4: The $C_2H_2$ + CO + H reaction network found in the experimental work by Qasim et al. (2019a). Figure taken from Qasim et al. (2019b), and originally adapted from Chuang et al. (2016).

COM formation starting from the OH radical has also been shown to be favorable. A number of alcohols, such as n- and i-propanol and n- and i-propenol, can be formed starting from the low energy barrier reaction of $C_3H_4$ and OH (Qasim et al. 2019c). Substituting $C_3H_4$ with $C_2H_2$ results in the products, acetaldehyde, vinyl alcohol, ketene, and ethanol (Chuang et al. 2020). As discussed in section 1.2.4, COMs have been detected in the gas-phase, that however are (partially) formed in the solid-state. How COMs, like the ones proposed here, can be released into the gas-phase in a non-thermal way is still an active research topic (Vasyunin & Herbst 2013; Bertin et al. 2016; Chuang et al. 2018b; Dartois et al. 2019).

### 1.2.6 Role of the James Webb Space Telescope for COMs

The James Webb Space Telescope (JWST), with a current expected launch date of March 2021, will be able to detect solid-state COMs that are more complex than $CH_3OH$ in dense clouds and dark cores – a feat that does not apply to current and previous observational facilities. Ice investigations of COMs in the Laboratory for Astrophysics and in other groups will be combined with chemical models and JWST observations of icy COMs to understand COM formation in various interstellar environments. Some of the advantages of using JWST to detect solid-state COMs in dark interstellar environments, as proposed in the MIRI Consortium and McClure et al. (2017), are briefly summarized below.

Space-based observatories have the advantage of complete wavelength coverage due to the absence of Earth's telluric contamination. However, previous space-based observatories, such as Spitzer and the Infrared Space Observatory (ISO), probed ices with low spectral resolution (Spitzer: R ~ 60-120) or low sensitivity (ISO). An example of blended ice features from Spitzer is shown in Figure 1.5.

Using JWST's NIRCam Wide Field Slitless Spectroscopy (WFSS) mode, a spectral resolution of ~1500 in the 2.5-5.0 μm region will be possible, which will allow separation of the broad infrared ice bands into distinct signatures (McClure et al. 2017). A S/N of 100 will be required to detect COMs at ~3.6 μm that are 3% of the continuum. For the 5-8 μm region, the MIRI medium-resolution spectrometer (MRS) will be used, which has R ~ 3000, to distinguish between less abundant COM species (McClure et al. 2017). A S/N of 300 will be needed, as the laboratory data predict COM features at only 1% of the continuum in this region. An additional advantage for ice observations with JWST is that an ice map with over 100 background stars can be covered at $A_V$ ~ 5-100 mags (McClure et al. 2017). To compare, the largest ice map created included only ten lines of sight (Pontoppidan et al. 2004). Such a map will not only expand the collection of sources with ice detections, but will also allow direct comparison of the ice composition and morphology from the edge of the cloud to its densest regions. The JWST Guaranteed Time Observations program, MIRI EC Protostars Survey (van Dishoeck et al. 2017), will provide complementary results to understanding the ice as well as gas-phase chemistry, particularly towards protostars.

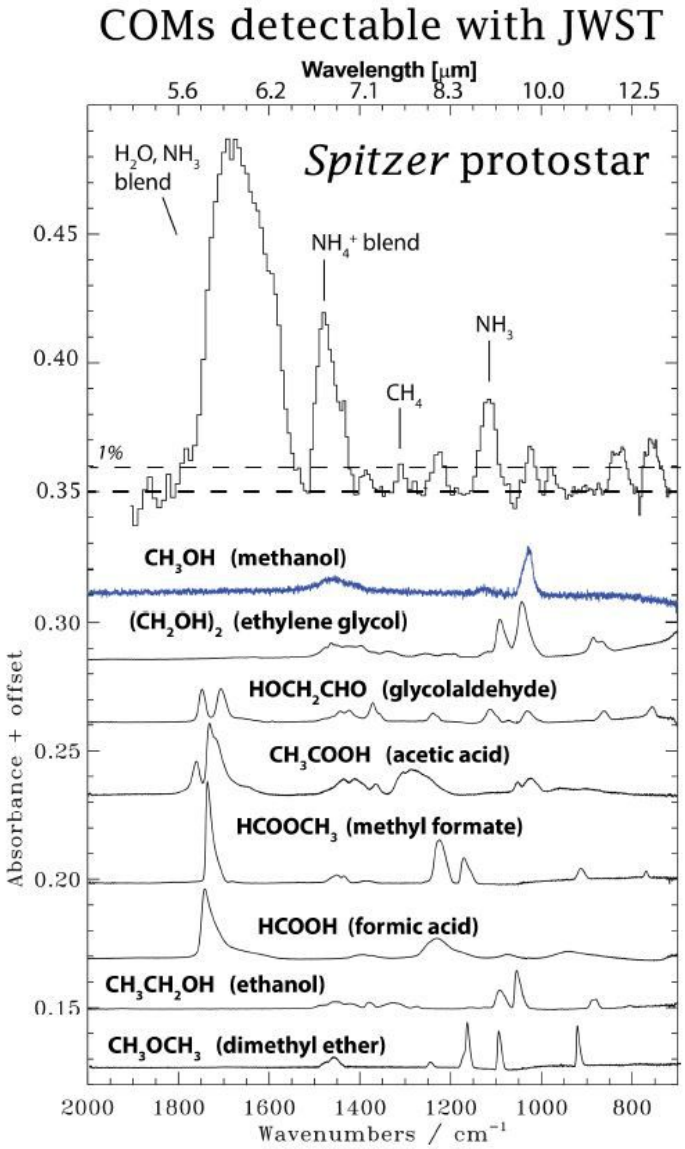


Figure 1.5: (Top) Spitzer ice spectrum taken towards RNO 90 (inverted, continuum and silicate subtracted), in which COMs are 1% of the continuum, requiring a S/N of 300 for detection. Beneath the Spitzer ice spectrum are laboratory solid-state infrared spectra of COMs. Unlike Spitzer, JWST will be able to spectrally resolve the infrared bands of COMs, although they still will be blended. Figure taken from McClure et al. (2017).

### 1.2.7 This thesis

In this era of astrochemistry, technological advances now allow us to delineate the physical and chemical properties of protoplanetary disks, which provide more clues as to how disks connect to planetary systems. But to fully understand how the disk came to be, knowledge of its birth place – the molecular cloud – is required. To date, there are still gaps in knowledge about the physics and chemistry of molecular clouds, and how the cloud transforms into a disk.

The aim of this thesis is to address the 'dark', or 'non-energetic', *ice* chemistry in molecular clouds/cores that is not thoroughly understood or even realized. The time frame that 'dark' ice chemistry peaks is thought to be the starting point at which a number of simple molecules and COMs are formed, typically on icy grain surfaces. Thus, the species formed in this phase are the starting ingredients to chemical evolution, from the clouds to nascent planets. Having a complete understanding of the initial ice chemistry will shed light to the chemistry in the next stages of stellar evolution.

To investigate such ices, laboratory simulations of realistic interstellar ice analogues are performed with SURFRESIDE$^3$ in the Leiden Laboratory for Astrophysics. To complement the laboratory work, astronomical observations are presented, along with quantum calculations to grasp the formation mechanism(s), relative abundances, and astrochemical relevance of each molecule studied. $CH_4$, which is the simplest molecule to be investigated, is observationally constrained to be formed from the sequential hydrogenation of solid C in the polar ice phase. It is experimentally shown that this is possible, which further validates the conclusions from observational surveys. This $CH_4$ can be a precursor to $CH_3OH$ formation, as shown in a dedicated laboratory paper on the reaction of $CH_4$ and OH. In turn, the findings from the laboratory paper are supported by a follow-up observational study of $CH_3OH$ ice towards numerous background stars. Other simple molecules, such as HCOOH and $CO_2$, are currently constrained to be formed largely from CO ice. Taking into consideration the abstraction of atoms, it is shown that reactions involving $H_2CO$ can also contribute to the solid-state inventory of HCOOH and $CO_2$. The formation of COMs, which is thought to occur once CO freezes out, is now experimentally constrained to take place also when $H_2O$ ice is formed – a time period earlier than expected. Alcohols and aldehydes are demonstrated to be possible ice constituents existing on top of carbonaceous grains. A larger variety of COMs, also to be formed in the $H_2O$-rich ice phase, is proposed in this thesis. Future work will involve COM formation in $H_2O$-rich ices starting from atomic C, a missing reaction channel in astrochemical models due to the lack of experimental studies. A summary of the aforementioned investigations divided into chapters is provided below.

**Chapter 2** details the experimental apparatus, SURFRESIDE$^3$, that is used in this thesis to study the 'non-energetic' formation of simple and complex organic molecules in interstellar clouds/cores. A background on the fundamentals of the experimental techniques, RAIRS and TPD, is provided, and how they are used in practice in SURFRESIDE$^3$ is discussed. The transition from SURFRESIDE$^2$ to SURFRESIDE$^3$, which mainly involves the addition of an atomic carbon source, is explicitly described. A separate vacuum apparatus is built to test and perform initial calibrations of the atomic carbon source. This

includes constraining the atomic carbon beam size to fit within the area of the substrate, and providing proof-of-concept experiments such as C + $^{18}O_2$, which shows the formation of C$^{18}$O and C$^{18}O_2$. With the C-atom source integrated into SURFRESIDE, atomic C fluxes of low $10^{11}$ - high $10^{12}$ cm$^{-2}$ s$^{-1}$ are measured, which are values high enough to probe C-atom induced chemistry in SURFRESIDE$^3$. These values are also complementary to the H-atom flux measured in SURFRESIDE$^3$, which should be higher than the C-atom flux in experiments in order to mimic the overabundance of H-atoms in comparison to C-atoms in interstellar clouds. SURFRESIDE$^3$ is the first experimental apparatus designed to study the formation of COMs starting from C-atoms in realistic interstellar ice analogues. Such COMs are expected to be most prevalent in the translucent phase ($H_2O$-rich ice phase) of interstellar clouds.

**Chapter 3** presents the first experimental study under controlled laboratory conditions of $CH_4$ formation in the way that it is observationally constrained to be formed: from the sequential hydrogenation of C in a $H_2O$-rich ice at low temperatures (~10 K). Not only is it proven that $CH_4$ can be formed in this way, but it is also shown that the formation rate is about twice as high compared to an experiment without water ($5.6 \times 10^{11}$ versus $3.5 \times 10^{11}$ molecules cm$^{-2}$ s$^{-1}$), which should be taken account into astrochemical models. The presence of water increases the residence time of hydrogen in the ice, thus increases the probability of hydrogen to react with carbon. The competing H-abstraction reactions by H-atoms are relatively ineffective compared to H-addition reactions under the presented experimental conditions, and are not expected to be effective on interstellar icy grains once $CH_3$ is formed in the reaction chain, thus providing a more secure route to $CH_4$ ice formation in the ISM. As $CH_4$ is best observed with space-based observatories, this study becomes timely with the anticipated launch of the JWST, which will have a sensitivity high enough to directly probe $CH_4$ in the $H_2O$-rich ices of quiescent clouds.

**Chapter 4** investigates another pathway to form $CH_3OH$ ice in interstellar clouds. This pathway starts from $CH_4$, which subsequently puts new constraints on the $CH_3OH$ ice formation threshold. Although H-abstraction from $CH_4$ using H-atoms is ineffective under cold interstellar cloud conditions, such an abstraction becomes more promising when OH-radicals are used, which results in the presence of $CH_3$ radicals that can react with OH to form $CH_3OH$. It is shown that this process works at 10 K, and is 20 times less efficient than the sequential hydrogenation of CO to form $CH_3OH$, which is the dominant pathway to $CH_3OH$ formation in interstellar clouds. This has two main consequences: 1) Since $CH_4$ ice is present before CO freezes out, this indicates that the $CH_3OH$ ice formation threshold should be below the CO freeze-out point. 2) The relative inefficiency of the $CH_4$ + OH route to form $CH_3OH$ may partially explain the low $CH_3OH$ upper limits found in observational surveys of background stars.

**Chapter 5** is a follow-up study on Chapter 4 from an observational perspective. To investigate whether $CH_3OH$ ice is initially formed when $CH_4$ ice is formed, a sample of 41 stars behind quiescent interstellar clouds/cores are observed at $A_V$ = 5.1 - 46.0 mags. To increase the sensitivity of the $CH_3OH$ ice feature at 3.537 μm, a method to reduce photospheric lines, and thus lower the upper limits, is demonstrated. As the JWST will also suffer from photospheric line contamination, this method can also be applied to future JWST

observations as well as to previously collected data. 1 new $CH_3OH$ ice detection is reported, which brings the total to 8 detections in quiescent environments. With this new detection, an updated $CH_3OH$ formation threshold of $A_V$ = $6.8 \pm 3.9$ mag is measured, which shows that more detections are still needed to confirm the threshold, as the value is only $1.7\sigma$. As only upper limits are measured below $A_V$ = 6.8 mag, this indicates that $CH_3OH$ is still constrained to be formed after $CH_4$ ice is formed. However, due to the large variations between upper limits and detections at high $A_V$, the possibility that less efficient, alternative pathways to $CH_3OH$ formation, such as the $CH_4$ + OH route, is still open.

**Chapter 6** demonstrates through experimental investigations coupled with computational calculations from the literature that HCOOH and $CO_2$ ices are formed in the CO-rich ice phase, in addition to the $H_2O$-rich ice phase. It is found that both, HCOOH and $CO_2$ can be formed starting from $H_2CO$, which is a product of the CO hydrogenation pathway. Starting from $H_2CO$, HCOOH is formed from two formation routes: H + HOCO and HCO + OH. $CO_2$ is predominantly formed from H + HOCO. It is suggested from the presented results that observational surveys targeting HCOOH ice, which has not been positively identified thus far, should probe within a certain $A_V$ range that is past the $H_2O$-rich ice phase and before $CH_3OH$ ice is sufficiently formed. This is because the overall abundance of HCOOH (and therefore the S/N) should be higher when probing deeper into the cloud/core, however probing too far may result in spectral signatures of $CH_3OH$ that may potentially overlap with those of HCOOH.

**Chapter 7** presents a study on the formation of propanal and 1-propanol under dark cloud conditions within the CO hydrogenation network. By adding hydrocarbon radicals to the network, COMs such as propanal and 1-propanol can be formed. Propanal is formed at the low temperature of 10 K by the reaction between HCO and $H_2CCH/H_3CCH_2$ radicals. 1-propanol is subsequently formed from the hydrogenation of propanal. From an activation barrier point of view, the pathway to propanal formation is promising in the ISM. The pathway to 1-propanol may be a minor route based on the presented activation energies, which however only represent some of the scenarios that may lead to 1-propanol formation from propanal hydrogenation. Atacama Large Millimeter/submillimeter Array (ALMA) observations towards the low-mass protostar, IRAS 16293-2422B, provide a 1-propanol:propanal upper limit ratio of < 0.35 - 0.55. This parallels the experimental work, as there should be less 1-propanol compared to propanal if 1-propanol is solely formed from the hydrogenation of propanal.

**Chapter 8** highlights that a number of alcohols can additionally be formed in the $H_2O$-rich ice phase of interstellar clouds, and likely with a higher efficiency depending on the starting materials chosen and their availability. Hydrocarbons ultimately originating from carbon-rich star environments, such as propyne ($H_3CC{\equiv}CH$), are expected to accrete onto carbonaceous dust grains that are formed from the nucleation of PAHs. It is demonstrated in a combined experimental and theoretical effort that propyne can react with nearby OH radicals formed in the $H_2O$-rich ice phase to produce an assortment of alcohols, including n- and i-propanol, n- and i-propenol, and potentially three isomers of propanediol. The n- and i-propanol abundance ratio of 1:1 aligns

with computational calculations that the barriers for propyne + OH to form both isomers are low, indicating that this reaction would be effective on icy dust grains if the reactants were next to each other on the surface. The findings are linked to the potential of forming astrobiological species, as polyynes containing $H_3C$-$(C{\equiv}C)_n$-H structures may transform into more complex alcohols, such as fatty alcohols, which are thought to have been components of primitive cell membranes.

## Bibliography


Agúndez, M. & Wakelam, V. 2013, Chem. Rev., 113, 8710

Allamandola, L., Sandford, S., & Valero, G. 1988, Icarus, 76, 225

Altwegg, K., Balsiger, H., & Fuselier, S. A. 2019, Annu. Rev. Astron. Astrophys., 57, 113

Arasa, C., van Hemert, M. C., van Dishoeck, E. F., & Kroes, G.-J. 2013, J. Phys. Chem. A, 117, 7064

Bacmann, A., Faure, A., & Berteaud, J. 2019, ACS Earth Space Chem.

Bacmann, A., Taquet, V., Faure, A., Kahane, C., & Ceccarelli, C. 2012, Astron. Astrophys., 541, L12

Balucani, N., Ceccarelli, C., & Taquet, V. 2015, Mon. Not. R. Astron. Soc. Lett., 449, L16

Bernstein, M. P., Dworkin, J. P., Sandford, S. A., Cooper, G. W., & Allamandola, L. J. 2002, Nature, 416, 401

Bertin, M., Romanzin, C., Doronin, M., et al. 2016, Astrophys. J. Lett., 817, L12

Boogert, A., Chiar, J., Knez, C., et al. 2013, Astrophys. J., 777, 73

Boogert, A., Gerakines, P. A., & Whittet, D. C. 2015, Annu. Rev. Astron. Astrophys., 53, 541

Boogert, A., Huard, T., Cook, A., et al. 2011, Astrophys. J., 729, 1

Broten, N., MacLeod, J., Avery, L., et al. 1984, Astrophys. J., 276, L25

Broten, N., Oka, T., Avery, L., MacLeod, J., & Kroto, H. 1978, Astrophys. J., 223, L105

Brünken, S., Gupta, H., Gottlieb, C., McCarthy, M., & Thaddeus, P. 2007, Astrophys. J. Lett., 664, L43

Cardelli, J. A., Clayton, G. C., & Mathis, J. S. 1989, Astrophys. J., 345, 245

Caro, G. M., Meierhenrich, U., Schutte, W., et al. 2002, Nature, 416, 403

Charnley, S., Kress, M., Tielens, A., & Millar, T. 1995, Astrophys. J., 448, 232

Charnley, S., Tielens, A., & Millar, T. 1992, Astrophys. J., 399, L71

Chiar, J., Adamson, A., Kerr, T., & Whittet, D. 1995, Astrophys. J., 455, 234

Chuang, K.-J., Fedoseev, G., Ioppolo, S., van Dishoeck, E. F., & Linnartz, H. 2016, Mon. Not. R. Astron. Soc., 455, 1702

Chuang, K.-J., Fedoseev, G., Qasim, D., et al. 2020, Astron. Astrophys.

Chuang, K.-J., Fedoseev, G., Qasim, D., et al. 2017, Mon. Not. R. Astron. Soc., 467, 2552

Chuang, K.-J., Fedoseev, G., Qasim, D., et al. 2018a, Astron. Astrophys., 617, 1

Chuang, K.-J., Fedoseev, G., Qasim, D., et al. 2018b, Astrophys. J., 853, 1

Chyba, C. & Sagan, C. 1997, in Comets and the Origin and Evolution of Life (Springer), 147–173

Cuppen, H., Ioppolo, S., Romanzin, C., & Linnartz, H. 2010, Phys. Chem. Chem. Phys., 12, 12077

Cuppen, H., van Dishoeck, E. F., Herbst, E., & Tielens, A. 2009, Astron. Astrophys., 508, 275

Dartois, E., Chabot, M., Barkach, T. I., et al. 2019, Astron. Astrophys., 627, A55

Dutrey, A., Guilloteau, S., & Guelin, M. 1997, Astron. Astrophys., 317, L55
Favre, C., Fedele, D., Semenov, D., et al. 2018, Astrophys. J. Lett., 862, L2
Fedoseev, G., Chuang, K.-J., Ioppolo, S., et al. 2017, Astrophys. J., 842, 1
Fedoseev, G., Cuppen, H. M., Ioppolo, S., Lamberts, T., & Linnartz, H. 2015, Mon. Not. R. Astron. Soc., 448, 1288
Fedoseev, G., Ioppolo, S., Zhao, D., Lamberts, T., & Linnartz, H. 2014, Mon. Not. R. Astron. Soc, 446, 439
Friberg, P., Madden, S., Hjalmarson, A., & Irvine, W. M. 1988, Astron. Astrophys., 195, 281
Fuchs, G., Cuppen, H., Ioppolo, S., et al. 2009, Astron. Astrophys., 505, 629
Garrod, R., Park, I. H., Caselli, P., & Herbst, E. 2006, Faraday Discuss., 133, 51
Garrod, R. T. & Pauly, T. 2011, Astrophys. J., 735, 15
Geppert, W. D., Hamberg, M., Thomas, R. D., et al. 2006, Faraday Discuss., 133, 177
Guidry, M. 2019, Stars and Stellar Processes (Cambridge University Press)
Guzmán, V. V., Pety, J., Gratier, P., et al. 2014, Faraday Discuss., 168, 103
Hama, T. & Watanabe, N. 2013, Chem. Rev., 113, 8783
Herbst, E. & Leung, C. M. 1989, Astrophys. J. Suppl. Ser., 69, 271
Herbst, E. & van Dishoeck, E. F. 2009, Annu. Rev. Astron. Astrophys., 47, 427
Ioppolo, S., Cuppen, H., Romanzin, C., van Dishoeck, E. F., & Linnartz, H. 2008, Astrophys. J., 686, 1474
Ioppolo, S., Cuppen, H., Romanzin, C., van Dishoeck, E. F., & Linnartz, H. 2010, Phys. Chem. Chem. Phys., 12, 12065
Ioppolo, S., Van Boheemen, Y., Cuppen, H., van Dishoeck, E. F., & Linnartz, H. 2011, Mon. Not. R. Astron. Soc., 413, 2281
Irvine, W., Hoglund, B., Friberg, P., Askne, J., & Ellder, J. 1981, Astrophys. J., 248, L113
Irvine, W. M., Brown, R., Cragg, D., et al. 1988, Astrophys. J., 335, L89
Jiménez-Serra, I., Vasyunin, A. I., Caselli, P., et al. 2016, Astrophys. J. Lett., 830, L6
Jørgensen, J., Schöier, F., & van Dishoeck, E. F. 2005, Astron. Astrophys., 435, 177
Jørgensen, J. K., Favre, C., Bisschop, S. E., et al. 2012, Astrophys. J. Lett., 757, L4
Jørgensen, J. K., van der Wiel, M., Coutens, A., et al. 2016, Astron. Astrophys., 595, A117
Kawaguchi, K., Kasai, Y., Ishikawa, S.-I., et al. 1994, Astrophys. J., 420, L95
Kennedy, G. M. & Kenyon, S. J. 2008, Astrophys. J., 673, 502
Kolasinski, K. W. 2012, Surface science: foundations of catalysis and nanoscience (West Chester, PA: John Wiley & Sons)
Kroto, H., Kirby, C., Walton, D., et al. 1977, in Bulletin of the American Astronomical Society, Vol. 9, 303
Langer, W., Velusamy, T., Kuiper, T., et al. 1997, Astrophys. J. Lett., 480, L63
Lee, J.-E., Lee, S., Baek, G., et al. 2019, Nat. Astron., 3, 314
Ligterink, N., Terwisscha van Scheltinga, J., Taquet, V., et al. 2018, Mon. Not. R. Astron. Soc., 480, 3628
Linnartz, H., Ioppolo, S., & Fedoseev, G. 2015, Int. Rev. Phys. Chem., 34, 205
Lovas, F. J., Remijan, A. J., Hollis, J., Jewell, P., & Snyder, L. E. 2006, Astrophys. J. Lett., 637, L37
Marcelino, N., Cernicharo, J., Agúndez, M., et al. 2007, Astrophys. J. Lett., 665, L127
Materese, C. K., Nuevo, M., & Sandford, S. A. 2017, Astrobiology, 17, 761
Matthews, H., Friberg, P., & Irvine, W. M. 1985, Astrophys. J., 290, 609
McCarthy, M., Gottlieb, C., Gupta, H., & Thaddeus, P. 2006, Astrophys. J. Lett., 652, L141
McClure, M., Bailey, J., Beck, T., et al. 2017, JWST Proposal ID 1309. Cycle 0 Early Release Science

McGuire, B. A., Burkhardt, A. M., Kalenskii, S., et al. 2018, Science, 359, 202
McGuire, B. A., Burkhardt, A. M., Shingledecker, C. N., et al. 2017, Astrophys. J. Lett., 843, L28
Meisner, J. & Kästner, J. 2016, Angew. Chem. Int. Ed., 55, 5400
Millar, T., Herbst, E., & Charnley, S. 1991, Astrophys. J., 369, 147
Millar, T. J. & Williams, D. A. 1993, Dust and chemistry in astronomy, Vol. 2 (CRC Press)
Öberg, K. I. 2016, Chem. Rev., 116, 9631
Öberg, K. I., Boogert, A., Pontoppidan, K. M., et al. 2011, Proc. IAU Symp. 280, 7, 65
Öberg, K. I., Garrod, R. T., van Dishoeck, E. F., & Linnartz, H. 2009, Astron. Astrophys., 504, 891
Öberg, K. I., Guzmán, V. V., Furuya, K., et al. 2015, Nature, 520, 198
Pontoppidan, K., van Dishoeck, E. F., & Dartois, E. 2004, Astron. Astrophys., 426, 925
Pontoppidan, K. M. 2006, Astron. Astrophys., 453, L47
Qasim, D., Fedoseev, G., Chuang, K. J., et al. 2020, An experimental study of the surface formation of methane in interstellar molecular clouds
Qasim, D., Fedoseev, G., Chuang, K.-J., et al. 2019a, Astron. Astrophys., 627, A1
Qasim, D., Fedoseev, G., Chuang, K.-J., et al. 2019b, arXiv preprint arXiv:1906.06508
Qasim, D., Fedoseev, G., Lamberts, T., et al. 2019c, ACS Earth Space Chem., 3, 986
Qasim, D., Lamberts, T., He, J., et al. 2019d, Astron. Astrophys., 626, A118
Remijan, A. J., Hollis, J., Snyder, L. E., Jewell, P., & Lovas, F. J. 2006, Astrophys. J. Lett., 643, L37
Shu, F. H., Adams, F. C., & Lizano, S. 1987, Annu. Rev. Astron. Astrophys., 25, 23
Snyder, L. E., Hollis, J., Jewell, P., Lovas, F. J., & Remijan, A. 2006, Astrophys. J., 647, 412
Soma, T., Sakai, N., Watanabe, Y., & Yamamoto, S. 2018, Astrophys. J., 854, 116
Suzuki, H., Ohishi, M., Kaifu, N., Ishikawa, S.-I., & Kasuga, T. 1986, Publ. Astron. Soc. Jpn., 38, 911
Terwisscha van Scheltinga, J., Ligterink, N., Boogert, A., van Dishoeck, E. F., & Linnartz, H. 2018, Astron. Astrophys., 611, A35
Thi, W.-F., Van Zadelhoff, G.-J., & van Dishoeck, E. F. 2004, Astron. Astrophys., 425, 955
van de Hulst, H. C. 1946, Recherches Astronomiques de l'observatoire d'Utrecht, 11, 2
van Dishoeck, E. F., Beuther, H., Caratti o Garatti, A., et al. 2017, JWST Proposal. Cycle 1, ID.# 1290
van Dishoeck, E. F., Blake, G. A., Draine, B. T., & Lunine, J. 1993, in Protostars and Planets III, 163–241
van´t Hoff, M. L., Tobin, J. J., Trapman, L., et al. 2018, Astrophys. J. Lett., 864, L23
Vasyunin, A. & Herbst, E. 2013, Astrophys. J., 769, 34
Walmsley, C., Jewell, P., Snyder, L., & Winnewisser, G. 1984, Astron. Astrophys., 134, L11
Ward-Thompson, D. 2002, Science, 295, 76
Watanabe, N. & Kouchi, A. 2002, Astrophys. J. Lett., 571, L173
Watson, W. & Salpeter, E. E. 1972, Astrophys. J., 174, 321
Whittet, D., Gerakines, P., Hough, J., & Shenoy, S. 2001, Astrophys. J., 547, 872
Wirström, E., Geppert, W. D., Hjalmarson, Å., et al. 2011, Astron. Astrophys., 533, A24